INTL JOURNAL OF ELECTRONICS AND TELECOMMUNICATIONS, 2011, VOL. 57, NO. 1, PP. 85–89
Manuscript received January 19, 2011; revised February 2011. DOI: 10.2478/v10177-011-0012-0

Bistatic Noise SAR Experiment with a Non-Cooperative Illuminator

Łukasz Maślikowski and Krzysztof Kulpa

***Abstract*—The paper describes the results of a conception-stage experiment with a ground-based bistatic noise SAR (Synthetic Aperture Radar) demonstrator. Its aim was to research the ability of a simple Commercial-Off-The-Shelf (COTS) build system to provide a bistatic SAR image using non-cooperative illuminator. The noise signal used in the experiment is similar to a signal used in many transmission systems such as DVB-T that can be employed in passive bistatic radars. The paper presents the system setup, details of the measurement campaign, signal processing and the results of SAR imaging.**

***Keywords*—SAR, noise radar, passive radar, COTS.**

I. Introduction

SYNTHETIC aperture radar is radar in which the sensor changes its position along the observed scene and soundings conducted for different sensor positions are treated as if they came from successive elements of a long antenna array. Such an array (synthetic aperture) can achieve very high directivity in the movement (azimuth) direction. Due to that, the minimal azimuth distance between two scatterers that can be still discerned (resolution) can be as small as L/2 in a focused case, where L is the antenna length in azimuth direction. The classical SAR systems use pulse illumination, which leads to small sidelobes in range dimension, but transmitted power must be relatively high – usually at the level of kilowatts. The alternative approach is to use continuous wave for scene illumination. The most popular technique in that case is to use linear frequency modulation – FMCW radar [1], [2]. The use of FMCW signals is appropriate only for short range radars, when range and Doppler ambiguities do not influence image formation. For longer ranges the interesting alternative is the noise SAR that uses noise or pseudo-noise signal for target illumination [3], [4]. The monostatic SAR systems are mature, but it is easy to detect, that the area is under scanning and to add false element to the scene using radio frequency memories [5]. The alternative way is to produce a SAR image of the terrain of interest using illuminators of opportunity [6], [7]. As the illuminators not only other SAR radars but also commercial transmitters with good ambiguity function, such as DAB and DVB-T, can be used. In such a case the transmitter is non-cooperative and to generate the image two signals have to be co-registered: measurement and reference one. The transmitted signal has rectangular spectrum and is very similar to the noise signal.

In most cases SAR system antennas are carried by a flying platform in order to image land surface [8]. However, SAR technique is also appropriate for imaging buildings, airport runways and so on when the sensor is mounted on a ground-based, moving platform. In such systems antenna platform may slide along rails [9] but there are also systems equipped with specially designed antennas with moving elements [10]. Ground based system is also a good platform for cheap emulation and testing of airborne system features and signal processing using real, measured data. The demonstrator built at Warsaw University of Technology, described in the paper, emulates a bistatic noise SAR system in which the stationary (non-moving) illuminator can either be regarded as a dedicated one or a completely non-cooperative unit, such as commercial radio, TV or GSM transmitter with analog or digital modulation. The first interpretation suits a bistatic active system while the second is the case for the passive one. The most promising modulations for passive SAR imaging are digital, noise-like signals, since wide signal spectrum results in a good range resolution (resolution along sounding). Growing number of such transmitters opens a way to employ them in passive SAR systems. An example of such system idea, that was a motivation for a ground-based experiment described in this paper, is presented in Fig. 1.

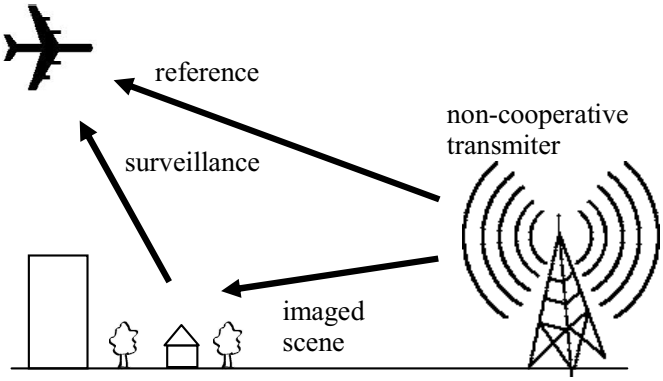

Fig. 1. An example operation diagram of a bistatic SAR system.

Moreover, the noise or noise-like continuous waveforms are now of great interest for radar engineers, since they can be used to obtain a SAR image with a low transmitted power (mean power of several mW up to several W). Such low power wideband signal does not interfere with other devices using the same bandwidth. While the noise signal is similar to one produced by thermal effects, it is hardly detectible and difficult to jam which brings obvious profits both in civil as well as military applications.

The authors are with the Institute of Electronic Systems, Warsaw University of Technology, Nowowiejska 15/19, 00-665 Warsaw, Poland (e-mails: L.Maslikowski@stud.elka.pw.edu.pl, kulpa@ise.pw.edu.pl).

Fig. 2. SAR trolley and the view of the observed scene.

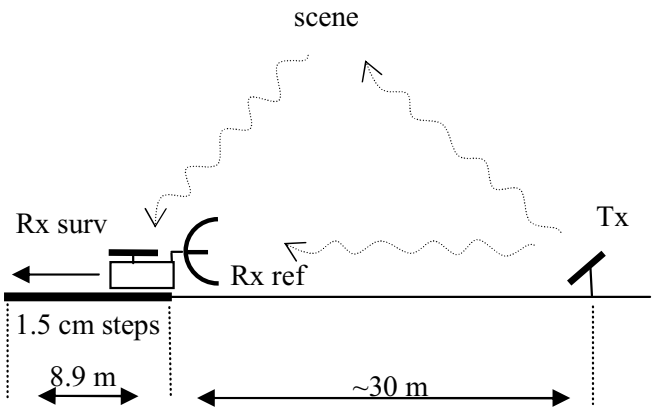

Fig. 3. The schematic diagram of the bistatic SAR experiment.

II. Bistatic SAR Demonstrator Setup

The transmitter site of the bistatic noise SAR demonstrator consisted of an arbitrary waveform generator (AWG) and a low-gain sector antenna that would illuminate the scene in a possibly uniform way. The AWG can generate the carrier frequency up to 2.6 GHz with arbitrary modulation defined by a complex baseband waveform previously uploaded into its memory. During the experiment a realization of Matlab generated white Gaussian noise with Gaussian spectrum was used. For the measurement the carrier frequency 2.3 GHz, as an interference-free, was selected. The I/Q DAC's clock frequency of the AWG is 60 MS/s, therefore the maximum signal bandwidth is 60 MHz, and a maximum output power is 26 dBm. The transmitter was placed on the balcony of the Warsaw University of Technology antenna laboratory, about 30 m from the receiver site. The reference signal was taken from the same antenna that illuminated the scene.

On the receiver site a two-channel vector signal analyzer (VSA) was used. The VSA converted the received signal to the I/Q baseband, sampled and recorded it. The instantaneous bandwidth of receiver is 36 MHz, and thus the bistatic range resolution is about 5 m. A high gain antenna directed at Tx antenna was used to gather possibly high-quality reference signal while the scene observation antenna was a wide-beam one. Both Rx antennas were placed on a small platform moving in the horizontal direction on the rails mounted on the DSP laboratory balcony, 20 m over the ground surface. The platform and the scene are presented in Fig. 2. The aim of the system was to simulate the airborne passive SAR; however, due to the limited number of stored samples in the memory of VSA it was not possible to record the signal continuously. To overcome this problem the system operated in a stop and-go-mode, which means that recordings were performed from stable positions of the antenna platform between its movements.

A step between antenna positions was equal to 1.5 cm (about 1/8 of the carrier wavelength) and the integration time was equal to 23 ms at each position. There were 600 antenna positions which correspond to 8.9 m synthetic aperture length. The exact distance between Rx and Tx antennas was measured with a laser rangefinder. The schematic diagram of the bistatic SAR experiment with non-cooperative illuminator is shown in Fig. 3.

III. Range Compression

The first stage of stop-and-go SAR signal processing is range compression performed for each sounding. Its aim is to cumulate the energy of the useful echoes in order to improve signal-to-noise ratio (SNR) and the range resolution. When the signal has wide bandwidth and unwanted noise is a Gaussian one, the optimal technique of compression is the matched filtering. In case of a random signal, predefined matched filter is not available so instead of a classical filtering cross-correlation between reference and surveillance signals is performed. From the mathematical point of view the result is the same.

A significant factor limiting dynamic performance of range compression in a noise radar may be the masking effect. Since the realization of a sounding signal is time and band limited, its autocorrelation (that in this case can be referred to as an ambiguity function) is not an ideal Dirac delta function. Due to band limitation, the correlation peak is wider than a delta function while due to the time window it has some non-zero values around its maximum. Those are known as the correlation processing floor or the residual fluctuations. The ratio of the power of the correlation peak to the fluctuations level is proportional to the signal bandwidth-time product which straightly corresponds to the number of correlated samples. That is the reason why a strong scatterer present in the scene can mask out any weaker echoes with its noise floor. In the described case there was no such strong dominant in the scene and the direct coupling between antennas was relatively small due to significant distance between Tx and Rx antennas. Thus, there was no need to use any direct signal cancellation methods such as adaptive filtering [11] that would decrease the processing floor.

The result of range compression is a matrix of range profiles. To present how the response of a single reflecting point is represented in such matrix a simulation of a scene

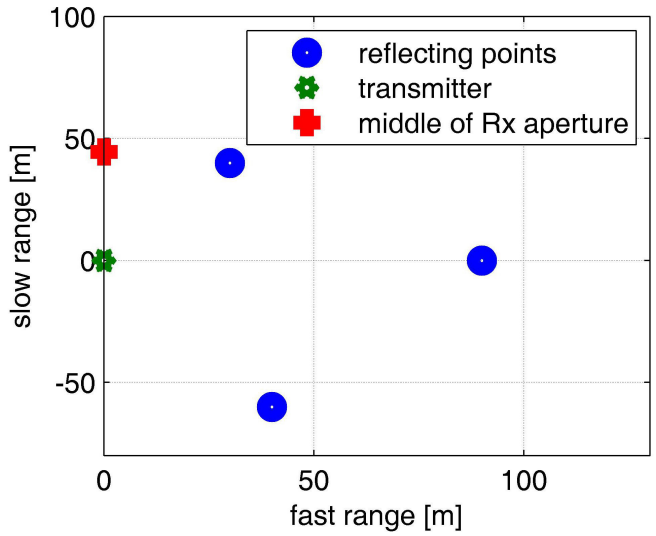

Fig. 4. The simulated scene setup.

with three point scatterers was conducted. The simulated scene setup was presented in Fig. 4.

One point was placed at smaller bistatic range while the two others at greater one, nearly equal for both of them but at different directions. The range profiles module was shown in Fig. 5. It is visible that the first scatterer produces nearly vertical line at delay of 5 samples while the two remaining points' responses are visible as an amplitude-modulated line at delay of 18. The modulation is a result of superposition of two responses which have different phase patterns. Responses produce nearly straight lines in this case but if the range resolution was better, range cell migration effect would be more distinct and lines would be slightly bend.

The range profiles matrix for a real scene was presented in Fig 6. There are strong reflections from the ground and nearby object visible as well as the echo of a huge building at delay of 20 – 25 samples. Due to Gaussian shape of the spectrum correlation sidelobes are hardly distinguishable.

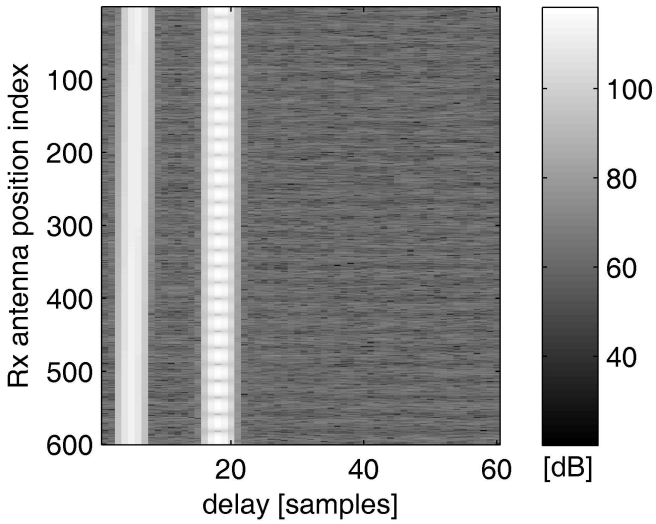

Fig. 5. The range profiles matrix of the simulated scene.

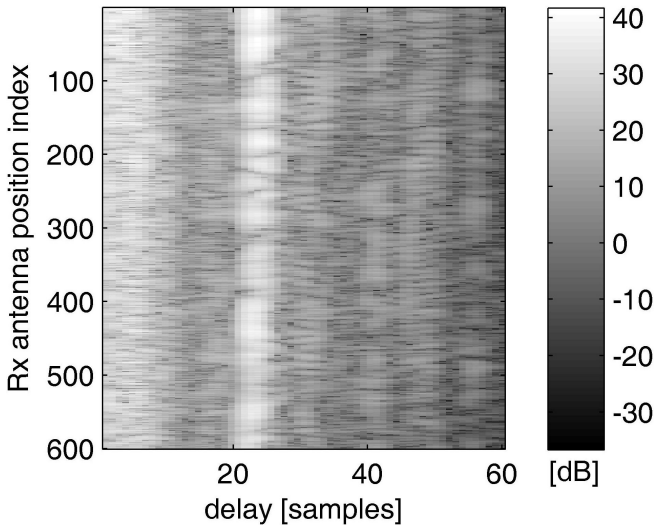

Fig. 6. The range profiles matrix of the real scene.

IV. Azimuth Compression

The second stage of processing is azimuth compression that transforms range profiles matrix into a SAR image. It uses phase dependencies between scatterer responses obtained for different antenna positions. In bistatic SAR those dependencies result from the geometry presented in Fig. 7.

A point-like scatterer is placed at coordinates (x, y), the transmitting antenna is placed at coordinates (x_{Tx}, 0), the receiving antenna is sliding on X axe and in the n-th position its coordinates are (x_{Rx}(n), 0). The echo signal reflected from the scatterer travels from the transmitting antenna to the receiving one and passes the distance:

$$r_{x,y}(n) = \sqrt{(x_{Tx} - x)^2 + y^2} + \sqrt{(x_{Rx}(n) - x)^2 + y^2}. \quad (1)$$

The reference signal travels from the transmitting antenna to the reference antenna passing the distance

$$r_b(n) = x_{Tx} - x_{Rx}(n) \quad (2)$$

Thus the delays between the signals are proportional to the difference of those two distances:

$$\Delta r_{x,y}(n) = r_{x,y}(n) - r_b(n) \quad (3)$$

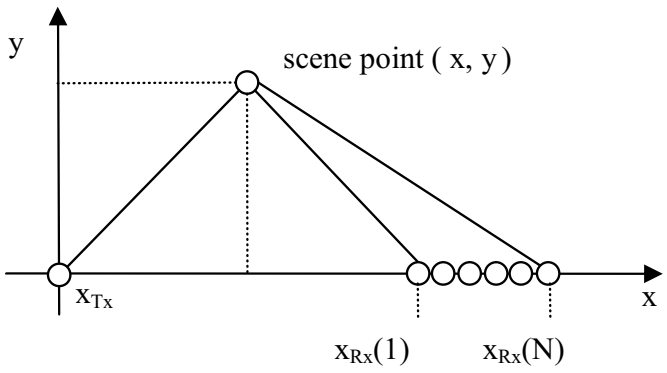

Fig. 7. The bistatic ground-based SAR geometry.

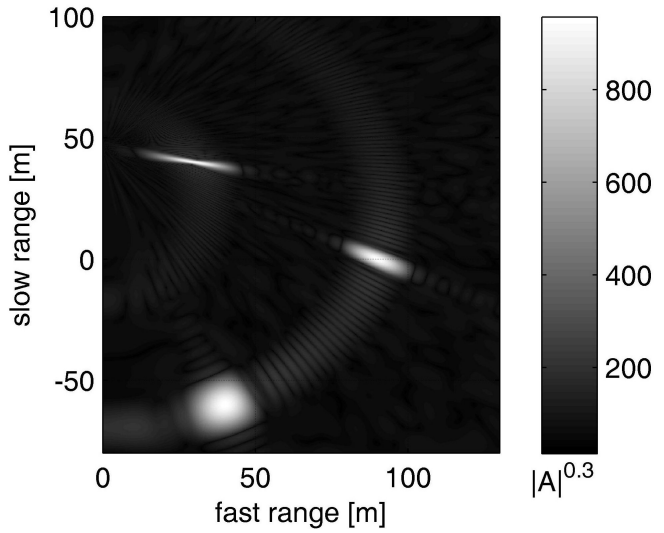

Fig. 8. Simulated SAR image.

and the phase shifts between the signals are equal to

$$\Delta\varphi_{x,y}(n) = \frac{2\pi}{\lambda}\Delta r_{x,y}(n) \tag{4}$$

where λ is the carrier wavelength. The phase pattern of the responses obtained from different antenna position is unique for each scatterer's position if only the Nyquist theorem is fulfilled in the azimuth domain. In this case it means that the steps between antenna position must be smaller than $\lambda/4$. That feature allows us to detect whether echo energy accumulated in range profiles comes from one scene point or another and lies at the basis of SAR imaging.

To produce the image the following procedure was performed. Firstly a rectangular grid in Cartesian coordinates was established so that each point of the grid represented one point of imaged scene (SAR image pixel). Then for each pixel a vector of differences $\Delta r_{x,y}(n)$ between distance Tx – scene point – Rx and Tx – Rx base was calculated using (3). Having those distances computed it was possible to perform Range Cell Migration Correction (RCMC). Distances in meters were transformed into appropriate values expressed in correlation samples. Then each row of range profiles was shifted so that the response from imaged point appeared in the first column of the matrix.

Finally matched filtering based on supposed pixel's response phase pattern was carried out:

$$A_{x,y} = \sum_{n=1}^{N} \exp(-j\Delta\varphi_{x,y}(n)) R_{x,y}(n) W(n) \tag{5}$$

where $A_{x,y}$ is a pixel complex value, N is a total number of antenna positions, $R_{x,y}(n)$ is a column of range profiles after Range Cell Migration Correction and W(n) is the applied window (e.g. Hamming window). At this stage matched filtering is performed rather than correlation since now range profiles, not noise signal realizations like in range compression, are processed and the filter pattern is strictly predefined for each pixel. Module of $A_{x,y}$ represents brightness of a SAR image pixel.

V. Processing Results

Results of SAR imaging of the simulated scene were presented in Fig 8. Echoes of three points presented in Fig. 4 are clearly visible. It is also visible that the azimuth resolution deteriorates when the object is placed far from the central axis of the synthetic aperture since the effective length of the aperture is small in such case.

The results of SAR processing and an optical image of observed scene are shown in Fig. 9. There is an echo of the huge building parallel to antenna rails visible. Between the building and antennas there are some trees and parked cars but at 36 MHz bandwidth they cannot be distinguished with high certainty.

VI. Conclusions

The goal of the presented research was to verify the possibility of SAR image creation using non-cooperative noise-like illuminator.

To simplify the hardware, bistatic noise SAR demonstrator was created using COTS elements such as arbitrary signal generator, vector analyzer, step motor and antenna systems used for WiFi. As the result the SAR image was created using non-cooperative noise waveform transmitter. Both the range resolution and cross range resolution was limited in the experiment. The range resolution was limited by the bandwidth of the signal. The cross-range resolution was limited by the length of synthetic aperture (length of the rails on the lab balcony).

In future it is planned to use the car or small airplane as the radar platform and record continuously DVB-T signals to simulate more realistic conditions.

References

[1] A. Meta, P. Hoogeboom, and L. P. Ligthart, "Signal Processing for FMCW SAR," *IEEE Transactions on Geoscience and Remote Sensing*, vol. 45, no. 11, pp. 3519–3532, November 2007.

[2] ——, "Range Non-linearities Correction in FMCW SAR," in *IEEE International Conference on Geoscience and Remote Sensing Symposium*, 31 July-4 August 2006, pp. 403–406.

[3] D. S. Garmatyuk and R. M. Narayanan, "Sar Imaging Using Acoherent Ultrawideband Random Noise Radar," in *Radar Processing, Technology, and Applications IV*, W. J. Miceli, Ed., vol. 3810, Denver, July 1999, pp. 223–230.

[4] K. Kulpa, "Space-borne Noise SAR – Performance Study," in *Proceedings of 6th European Conference on Synthetic Aperture Radar*, Dresden, Germany, 16-18 May 2006, p. 4.

[5] M. Soumekh, "SAR-ECCM Using Phase-Perturbed LFM Chirp Signals and DRFM Repeat Jammer Penalization," in *International Radar Conference*, 9-12 May 2005, pp. 507–512.

[6] S. Serva, F. Colone, and P. Lombardo, "A Study for a Space-Based Passive Multi-Channel SAR," in *IEEE Aerospace Conference*, 3-10 March 2007, pp. 1–11.

[7] K.-H. Liu and D. C. Munson, "Autofocus in Multistatic Passive SAR Imaging," in *IEEE International Conference on Acoustics, Speech and Signal Processing*, 31 March-4 April 2008, pp. 1277–1280.

[8] H. Wuming and W. Jun, "Airborne SAR Passive Radar Imaging Algorithm Based on External Illuminator," in *1st Asian and Pacific Conference on Synthetic Aperture Radar*, Huangshan, China, 5-9 November 2007, pp. 642–645.

[9] W. Nel, J. Tait, R. T. Lord, and A. J. Wilkinson, "The Use of a Frequency Domain Stepped Frequency Technique to Obtain High Range Resolution on the CSIR X-Band SAR System," in *Proceedings of 6th Africon Conference in Africa*, George, South Africa, October 2002, pp. 327–332.

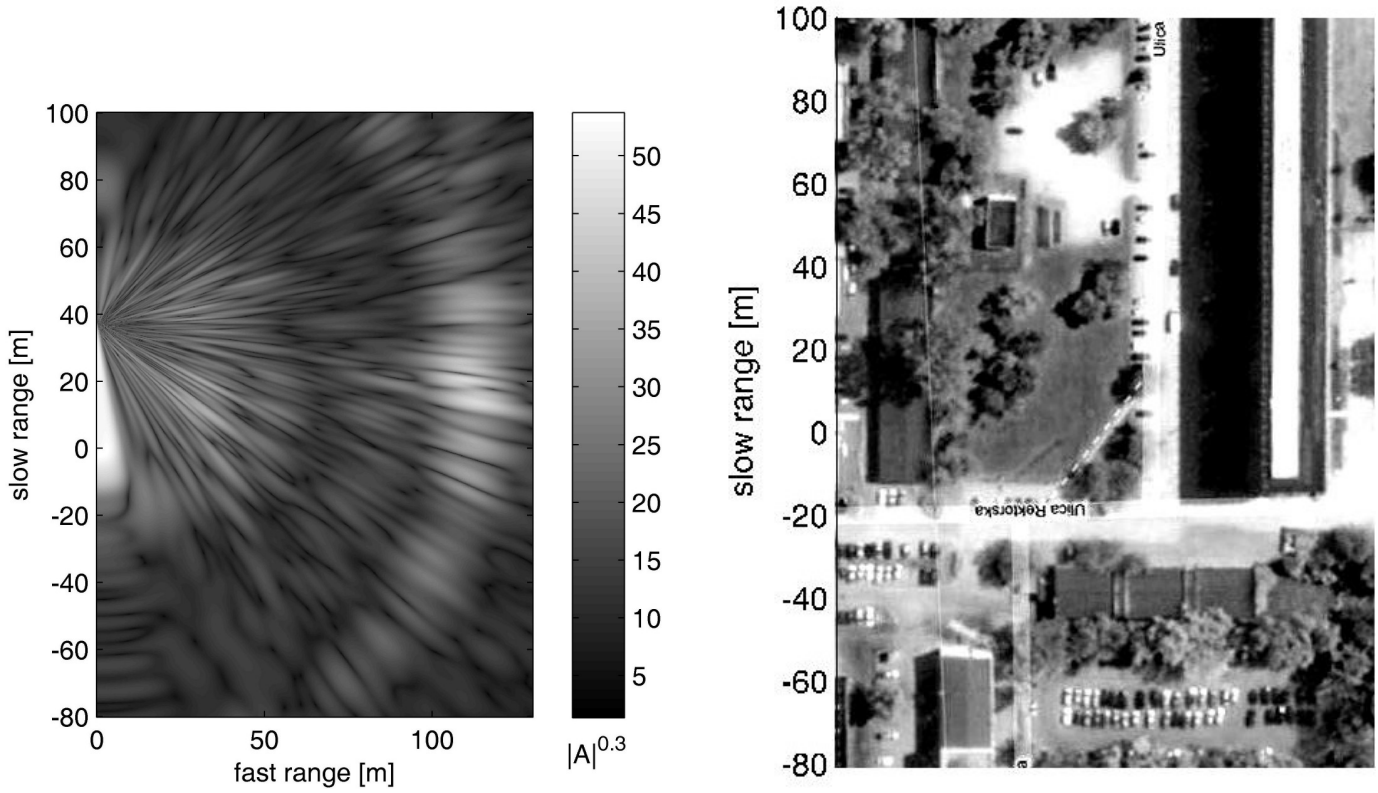

Fig. 9. SAR image and optical image of the real scene.

[10] K. A. Lukin [et all], "Ka-band Bistatic Ground Based Noise-Waveform-SAR," in *Proceedings of International Radar Ssmposium*, Wrocław, Poland, 21-23 May 2008, pp. 147–150.

[11] K. S. Kulpa and Z. Czekala, "Ground Clutter Suppression in Noise Radar," in *Proceedings of International Conference RADAR*, Tuluse, France, 18-22 October 2004, pp. 236–240.

[12] K. A. Lukin, "Ground Based Noise-waveform SAR for Monitoring of Chernobyl Sarcophagus," in *Proceedings of International Radar Symposium*, Berlin, Germany, 6-8 September 2005, pp. 655–659.

[13] B. M. Horton, "Noise-Modulated Distance Measuring System," *Proceedings of the Institute of Radio Engineers*, vol. 47, pp. 821–828, May 1959.

[14] G. R. Cooper and C. D. McGillem, "Random Signal Radar," School of Electrical Engineering, Purdue University, Final Report TREE67-11, June 1967.